AL
ory
n Laboratory

RAL Report
RAL-94-104

hep

Parton Distributions for Low Q^2

A D Martin W J Stirling and R G Roberts

September 1994

Rutherford Appleton Laboratory Chilton DIDCOT Oxfordshire OX11 0QX

DRAL is part of the Engineering and Physical Sciences Research Council

RAL-94-104
DTP/94/78
September 1994

Parton Distributions for low Q^2

A.D. Martin and W.J. Stirling

Department of Physics, University of Durham
Durham DH1 3LE, England

and

R.G. Roberts

Rutherford Appleton Laboratory,
Chilton, Didcot OX11 0QX, England

Abstract

We extend the MRS(A) set of parton distributions, which provides an up-to-date description of the structure of the proton probed by hard interactions, into the region of Q^2 below 5 GeV^2. After physically-motivated modifications, we obtain a smooth description of the data on the structure function $F_2(x, Q^2)$ all the way from $Q^2 = 10^{-1}$ to 10^3 GeV^2.

1 Introduction

Perturbative QCD is remarkably successful in describing a broad sweep of hard-scattering processes involving the nucleon. This implies that it is possible to extract from the data a consistent set of parton distributions in the proton, $f_i(x,Q^2)$, which evolve in Q^2 according to the standard GLAP equations in the region where perturbative QCD is appropriate.

Experimentally there has been steady progress, first in extending the kinematic range and in improving the precision of the data (in particular of the deep-inelastic structure function measurements) and, secondly, in extending the range of "hard" scattering data (e.g. the recent measurements of the $W^{\pm}$ rapidity asymmetry [1] and of the asymmetry in Drell-Yan production in pp and pn collisions [2]). As a result, modern sets of parton distributions [3, 4, 5] are strongly constrained. Here we concentrate on the most recent set of partons, MRS(A) [5], which were obtained in a global analysis of the full range of deep-inelastic and related data. These distributions provide a detailed description of the proton structure in the region where leading-twist perturbative QCD is valid, which may be taken as $Q^2 > Q_0^2 \approx 4$ GeV^2. In the case of deep-inelastic scattering, we know that higher-twist contributions become important even above this value of Q^2, especially at large x, and so an additional cut is always made in W^2, typically $W^2 > W_0^2 \simeq 10$ GeV^2.

There are, however, good reasons for requiring a quantitative description of the nucleon structure at lower values of Q^2. In structure function measurements, for example, the implementation of radiative corrections requires an approximate description of F_2 at low Q^2. Indeed, there now exist several low-Q^2 parametric forms for $F_2(x,Q^2)$ [6, 7, 8, 9, 10] which accurately describe F_2 in a restricted region of Q^2 and x. An excellent summary of the situation has recently been presented by Badelek and Kwiecinski [11]. There is also a demand for *individual* parton distributions $f_i(x,Q^2)$ valid at low Q^2 as well as for $Q^2 > Q_0^2$. For example, many of the measurements at HERA involve the use of Monte Carlo event generators which describe parton showering down to really low Q^2 values.

The aim of this paper is to provide a set of parton distributions that is consistent with the data taken at low Q^2 (down to $Q^2 \simeq 0.1$ GeV^2) and, as Q^2 rises, smoothly approaches the set MRS(A) which is consistent with the high-Q^2 experimental data. Note that there is already one set of parton distributions, that of Gluck, Reya and Vogt (GRV) [12], which could, in principle, be used down to $Q^2 = 0.3$ GeV^2. Their procedure is to start with a set of 'valence'-like quark and gluon distributions at $\mu^2 = 0.3$ GeV^2 and to evolve these up in Q^2 using the standard leading-twist (= 2) next-to-leading-order evolution equations. Above $Q^2 = O(2$ GeV$^2)$ these provide a reasonable description of F_2, consistent with the belief that, by then, the twist-two component

is expected to dominate. At low Q^2, however, the higher-twist contributions are important and the GRV partons alone do not give a good description of F_2 there, as was never their intention. Moreover, there are also concerns that the perturbative GLAP evolution of valence-like GRV partons at small x and Q^2 is unreliable [13].

In contrast, what we provide here are 'effective' low-Q^2 parton distributions which are modified versions of the leading-twist distributions, i.e. they satisfy leading-twist Q^2 evolution only for $Q^2 \gtrsim 5$ GeV^2. In other words, the unknown higher-twist and non-perturbative components are the origin of the empirical Q^2 modifications we impose on the distributions at low Q^2, such that when these partons are inserted into the formal expressions for F_2, we obtain detailed agreement with the data. Particularly useful in this context are the new low-Q^2 structure function measurements from the E665 collaboration [14].

Note that the gluon and sea-quark distributions of the MRS(A) set of partons have the singular small-x behaviour

$$xg,\ xq_{\rm sea} \sim x^{-0.3} \tag{1}$$

as $x \to 0$, which results from including the HERA measurements of F_2 in the global analysis. For such a singular gluon distribution, GLAP evolution is expected [13, 15] to faithfully mimic the small-x description of F_2 by the BFKL equation [16].

2 Parametrization of partons at low Q^2

Our starting point is the MRS(A) set of parton distributions, which are obtained from a global data analysis of deep-inelastic and related data with $Q^2 > 5$ GeV^2 (and $W^2 > 10$ GeV^2). The partons give an excellent description of these data. However our goal here is to obtain partons which describe data to much lower values of Q^2 (and W^2). We therefore begin by using the next-to-leading-order GLAP equations to evolve down in Q^2 from the MRS(A) starting distributions at $Q_0^2 = 4$ GeV^2. At some stage we anticipate that such a leading-twist GLAP-based extrapolation will fail. Note that as we go below the charm threshold, the number of active flavours in the evolution drops from 4 to 3, and from our previous analysis [5] this threshold is taken at $Q^2 = m_c^2 = 2.7$ GeV^2.

First we must allow for the effects of the target mass, which were not included in the MRS(A) analysis. Such effects do not so much concern low-x data (where the photon-proton scattering energy is large) but rather apply to data at large x where they are significant even for $Q^2 \gtrsim 10$ GeV^2. Data in this kinematic region were excluded from the MRS(A) analysis by the W^2 cut and so did not distort the fit. To include the target mass corrections we replace x by the target mass variable

ξ [17], where

$$\xi = \frac{2x}{1+r} \quad \text{with} \quad r^2 = 1 + \frac{4M^2x^2}{Q^2} \tag{2}$$

where M is the mass of the target. From Fig. 1 we see that this straightforward correction gives a dramatic improvement in the description of the large x SLAC measurements of F_2 [18]. Here the difference between the modified and unmodified data is almost entirely due to the $x \to \xi$ substitution.

Our primary interest is the behaviour at low Q^2. There exist fixed-target measurements of $F_2(x,Q^2)$ at low Q^2 and low x. Indeed, the E665 collaboration have recently presented preliminary data which access even lower Q^2 and x values than hitherto. We expect that $F_2(x,Q^2)$ reconstructed from MRS(A) partons evolved to low Q^2 will, at some stage in the backwards evolution, begin to overshoot the data, since the fundamental requirement that

$$F_2 \to O(Q^2) \tag{3}$$

as $Q^2 \to 0$ is not embodied in the perturbative QCD evolution. The most natural way to rectify this deficiency is to introduce a form factor

$$\rho(x,Q^2) = \frac{Q^2}{Q^2+m^2} \tag{4}$$

into the parton distributions, where the x dependence of m^2 is to be determined from the low-Q^2 data. In this way we achieve a phenomenological description of higher-twist contributions which may, for example, arise from parton shadowing [20]. If the latter is the dominant higher-twist effect, we would expect m^2 to increase with decreasing x, as can be seen from the following simple argument. Naively, we would expect shadowing to become important when the total gg 'interaction area' becomes a significant fraction of the transverse area (πR^2) in which the gluons are confined within the proton. That is when

$$\frac{n_g \sigma_{gg}}{\pi R^2} \sim O(\alpha_s)\,, \tag{5}$$

where $n_g \sim xg$ is the gluon density per unit rapidity. Noting that $\sigma_{gg} \sim \alpha_s^2/Q^2$, this implies that the 'critical line' in the $(Q^2, 1/x)$ plot for the onset of shadowing has the form

$$Q^2 \sim m^2 \sim x^{-\lambda} \tag{6}$$

where, for simplicity, we have assumed $xg, x\bar{q} \sim x^{-\lambda}$ and ignored the running of α_s.

In practice it is clearly desirable to distort the MRS(A) partons as little as possible for $Q^2 > Q_0^2 \equiv 4$ GeV^2, and so we choose

$$m^2 = m_0^2(x)\, \exp(-Q^2/Q_0^2)\,. \tag{7}$$

Thus there is negligible modification to the partons (i.e. $\rho \simeq 1$) in the kinematic region ($Q^2 > Q_0^2$) of the data that originally determined the MRS(A) distributions. The exponential factor in (7) does not significantly distort the determination of the x dependence of m^2, since m^2 is mainly determined by F_2 data with $Q^2 \lesssim 1$ GeV^2.

In summary, we modify the evolved MRS(A) parton distributions so that they take the form

$$f_i(x,Q^2) = \rho(x,Q^2)\, f_i^{\rm MRSA}(\xi,Q^2)\,, \tag{8}$$

and determine the parameter m_0^2 in ρ by fitting to the $F_2(x,Q^2)$ data at low Q^2 for each value of x. It is interesting to note that the form factor modification and the $x \to \xi$ target mass correction essentially decouple as they are relevant in distinct kinematic regimes, namely in low-Q^2, low-x and in large-x, moderate-Q^2 regions respectively.

In principle it could be argued that a different form factor should be used for different parton distributions. However the low-Q^2, low-x data are dominantly described by the sea-quark distributions. For instance, we find no significant change in the results if we use an unmodified distribution for the gluon, that is $\rho = 1$. (Computing the value of $R = \sigma_L/\sigma_T$ using the QCD expression for F_L evaluated with our modified distributions does not remove the discrepancy between the SLAC data [18] and the QCD prediction. The values of R obtained by SLAC still tend to lie above the computed values.)

Finally we note a small technical point. When the MRS(A) parton distributions are evolved down from $Q_0^2 = 4$ GeV^2, the gluon distribution $xg(x,Q^2)$ begins to become negative over a small range of moderate x, just below $Q^2 = 0.625$ GeV^2. We therefore freeze the unmodified partons, $f_i^{\rm MRSA}(x,Q^2)$, for $Q^2 < 0.625$ GeV^2 at their values at $Q^2 = 0.625$ GeV^2, i.e.

$$Q^2 \to Q^2 + (Q_c^2 - Q^2)\theta(Q_c^2 - Q^2) \tag{9}$$

in the argument of the $f_i^{\rm MRSA}$, with $Q_c^2 = 0.625$ GeV^2. The effect on the behaviour of the u sea-quark distribution is shown in Fig. 2 for two relevant values of x. Since the unmodified distributions are decreasing only slowly with Q^2 there is little effect on the description of F_2.

3 The description of F_2^p data at low Q^2

The behaviour of the parameter $m^2(x)$ as a function of x is determined by fitting to the F_2 data of E665 [14] and SLAC [18], and also the 90 GeV data of NMC [21]. The NMC data for $Q^2 > 5$ GeV^2 proved to be crucial in constraining the MRS(A) partons. Although in principle the overall normalization of the NMC data could be

varied with respect to the other data sets, no correction was in fact needed [5]. When we include the E665 data in our analysis we again allow for an arbitrary relative normalization adjustment. There is in fact a significant overlap in the x, Q^2 ranges of the NMC and E665 data sets and we find that consistency is achieved if the latter are renormalized up by 20%. Although this may appear to be a large factor, the E665 data are still preliminary, with a figure of 10-20% being quoted as the typical systematic uncertainty [14]. Applying this correction factor 1.2 to the E665 data leads to a systematic x dependence in the values of $m_0^2(x)$ extracted from F_2 measurements of the three experiments, SLAC, NMC and E665.

The results are shown on a $\log m_0^2 - \log x$ plot in Fig. 3(a), and indicate that a good fit to the x dependence of m_0^2 can be obtained by using the form

$$m_0^2(x) = Ax^{-n} \,. \tag{10}$$

We find $A = 0.07$ GeV^2 and $n = 0.37$, corresponding to the straight line in Fig. 3(a). It is remarkable that the $x^{-0.37}$ behaviour obtained from low-Q^2 data is compatible with the observed singular $x^{-0.3}$ gluon and sea-quark small-x behaviour, (1), obtained from large Q^2 data. This connection between independent results obtained from different kinematic regions is suggested by the simple arguments which lead to (6). It is interesting to note that $m_0^2(x)$ could be equally well by represented by the alternative form

$$m_0^2(x) = A \exp\left[B\sqrt{\ln\left(\frac{1}{x}\right)} \right] \,. \tag{11}$$

as shown in Fig. 3(b). The straight line corresponds to $A = 0.015$ GeV^2 and $B = 1.54$ in (11). Note that the quoted values for A and n in (10) are for fits are performed in the $\overline{\rm MS}$ scheme. A similar fit in the DIS factorization scheme gives $A = 0.055$ GeV^2 and $n = 0.39$.

In Figs. 4 and 5 we show the description of the low-Q^2 measurements of F_2 [14, 18, 21] using the MRS(A) partons modified as in (8) with m_0^2 given by (10). In Fig. 6 we show, at sample values of x, the continuation of the low-Q^2 description to the recent HERA measurements of F_2 [22, 23]. The continuous curves show that the partons give a good description of F_2 throughout the range $10^{-1} \lesssim Q^2 \lesssim 10^3$ GeV^2. The predictions of the 'dynamical' GRV partons [12] are also shown (by dotted curves) in Fig. 6. Within the scope of their model, these partons provide an excellent description of F_2 for $Q^2 \gtrsim 1$ GeV^2 but below this value increasingly undershoot the data. It can also be glimpsed from Fig. 6 that the recent HERA data indicate that the GRV predictions increase a little too steeply with decreasing x.

4 F_2^n at low Q^2

There is also evidence for higher-twist corrections from SLAC and NMC low-Q^2 data [24, 25] for the ratio of the neutron and proton structure functions. The deviations from the MRS(A) perturbative QCD predictions for F_2^n/F_2^p occur in the interval $x \sim 0.1$ to 0.3 and so we introduce a further modification to the *valence* quarks solely to describe these deviations.[1] We use the following simple one-parameter form which allows F_2^n to be varied at low Q^2 while leaving F_2^p unaffected:

$$\begin{aligned} u_v(x,Q^2) &\rightarrow u_v'(x,Q^2) = (1-\frac{r}{4})u_v(x,Q^2) - \frac{r}{4}d_v(x,Q^2) \\ d_v(x,Q^2) &\rightarrow d_v'(x,Q^2) = (1+r)d_v(x,Q^2) + ru_v(x,Q^2) \end{aligned} \tag{12}$$

where

$$r = \frac{\tilde{Q}^2}{Q^2+\tilde{Q}^2}\,. \tag{13}$$

The F_2^n/F_2^p data obtained by NMC are shown in Fig. 7. They have been corrected for deuteron shadowing effects using the results of the analysis of [26]. We see that the predictions obtained from the MRS(A) partons (continuous curves) tend to undershoot the data. This discrepancy, however, is much less than for F_2^p itself at low Q^2, as would be expected for the ratio F_2^n/F_2^p which depends primarily on the valence distributions. The dashed curves, obtained using Eqs. (12) and (13) with $\tilde{Q}^2 = 0.12$ GeV^2, give a good description of the data. Whether this simple parametrization is adequate for smaller values of Q^2 is not certain. In any case, *nuclear* shadowing at such low Q^2 is expected to overwhelm such a simple partonic description.

In Fig. 8 we show the prediction of the modified MRS(A) partons (continuous curves) for the EMC(NA28) [27] measurement of F_2 on a deuterium target. In this case the curves (and not the data) have been corrected for deuterium screening effects. The description is very satisfactory and mainly checks the form factor modification of (8). These data are not sufficiently precise to further constrain the parameter r in (12), since the valence-quark contribution is small for those EMC data which lie at low Q^2. For comparison, we also show the GRV predictions for F_2^D. At $Q^2 = 0.35$ GeV^2 the GRV values are about a factor 2 below the data, but very rapidly evolve upwards with increasing Q^2 to be in reasonable agreement with the data.

[1] Note that the flavour-independent form factor modification of Eq. (8) would leave the F_2^n/F_2^p ratio essentially unchanged.

5 Conclusions

A low-Q^2 parton model is really a contradiction in terms. At some stage as Q^2 decreases, the description of the proton's structure cannot be expressed in terms of single parton densities with simple logarithmic behaviour in Q^2. The contributions from parton-parton correlation densities with power behaviour must enter and eventually the non-perturbative behaviour dominates. Moreover, all of these contributions are expected to be process-dependent. The set of distributions we have derived in this study correspond to what we may call 'effective' partons, insofar as power-law corrections like those introduced in Eq. (8) would presumably arise from including gluon-quark or quark-antiquark correlation distribution functions. In the framework of the operator product expansion, we assume that these higher-twist terms can be added to the leading-twist piece, each with their separate Q^2 dependence. These effective partons do not of course satisfy the usual conservation laws – number of valence quarks, total fractional momentum, etc. – but the violation is below 20% even for $Q^2 \sim 0.5$ GeV^2. Their detailed structure at low Q^2 is also very dependent on the precise form of the starting distributions at $Q_0^2 = 4$ GeV^2. Note that, in contrast with the studies in Refs. [6, 7, 8, 9, 10], we are not attempting here to make a model which has a smooth transition to the $Q^2 \to 0$ photoproduction limit, where a parton-based approach is clearly invalid.

From our study we may estimate, at least in the case of 'singular' MRS-type parametrizations, where the leading-twist GLAP evolution begins to become unreliable as Q^2 decreases. Interestingly, this depends on the value of x in just such a way as if the higher-twist contribution arose from parton shadowing. Some insight may be obtained by presenting the results as a function of x at fixed Q^2. In Fig. 9 we display this dependence of the F_2^p and F_2^D data for $Q^2 \simeq 0.3$ GeV^2. In this low-Q^2 regime the data are reasonably flat, whereas we see that the unmodified MRS(A) partons (dashed curves) partly retain the $x^{-0.3}$ behaviour of the distributions at the start of the backward evolution. The higher-twist, form-factor modification (continuous curves) restores the agreement with the data, with the modification decreasing as x increases. These data indicate large higher-twist contributions, but as Q^2 increases towards 5 GeV^2 these effects rapidly decrease.

Backward evolution in Q^2 is much more sensitive to the starting distributions than is forward evolution. It is therefore possible to conceive 'non-singular' starting parametrizations (with a lower starting scale Q_0) in which the higher-twist effects estimated in this way are much smaller. In this case the rise in F_2 with decreasing x seen at HERA is generated by the long evolution length. The GRV partons [12] are a parametrization of this type. We show in Fig. 9 the GRV predictions, which at this value of Q^2 undershoot the data with a shape which reflects their valence-like input

at $Q^2 = 0.3$ GeV^2. With increasing Q^2, the agreement between the GRV description and the data rapidly improves (see Fig. 6).

Our justification for discussing individual parton distributions at very low Q^2 values is largely practical. As mentioned earlier, parton showering Monte-Carlo programs at HERA incorporate parton densities at some low cut-off in Q^2. We are providing here effective parton densities which, when substituted into the next-to-leading-order expressions for $F_2(x, Q^2)$, give a reliable description of the data down to $Q^2 = 10^{-1}$ GeV^2 and, on the other hand, up to $Q^2 = 10^3$ GeV^2.[2] Fig. 6 shows how $F_2(x, Q^2)$ for small values of x is well described throughout all of this region.

Acknowledgements

We thank Jan Kwiecinski and Genya Levin for valuable discussions, and Heidi Schellman for information concerning the E665 experiment.

References

[1] CDF collaboration: A. Bodek, Proc. of International Workshop on Deep-Inelastic Scattering, Eilat, Israel, February 1994.

[2] NA51 collaboration: A. Baldit *et al.*, Phys. Lett. **B332** (1994) 244.

[3] A.D. Martin, R.G. Roberts and W.J. Stirling, Phys. Lett. **B306** (1993) 145.

[4] CTEQ collaboration: J. Botts *et al.*, Phys. Lett. **B304** (1993) 159.

[5] A.D. Martin, R.G. Roberts and W.J. Stirling, University of Durham preprint DTP/94/34, RAL report RAL-94-055, to be published in Phys. Rev. **D**.

[6] B. Badelek and J. Kwiecinski, Zeit. Phys. **C43** (1989) 251; Phys. Lett. **B295** (1992) 263.

[7] H. Abramowicz, E.M. Levin, A. Levy and U. Maor, Phys. Lett. **B269** (1991) 465.

[8] NMC: P. Amaudruz *et al.*, Nucl. Phys. **B371** (1992) 3.

[9] A. Donnachie and P.V. Landshoff, Zeit. Phys. **C61** (1994) 139.

[2] The **FORTRAN** code for the distributions, in both the $\overline{\text{MS}}$ and DIS factorization schemes, can be obtained by electronic mail from W.J.Stirling@durham.ac.uk

[10] A. Capella, A. Kaidalov, C. Merino and J. Tran Thanh Van, Orsay preprint LPTHE 94-34 (1994).

[11] B. Badelek and J. Kwiecinski, Warsaw preprint IFD/1/1994.

[12] M. Glück, E. Reya and A. Vogt, Zeit. Phys. **C53** (1992) 127; Phys. Lett. **B306** (1993) 391.
M. Glück and E. Reya, Dortmund preprint DO-TH 93/27 (1993).

[13] R.K. Ellis, Z. Kunszt and E.M. Levin, Nucl. Phys. **B420** (1994) 517.

[14] E665 collaboration: presented by A.V. Kotwal at the VIth Rencontre de Blois, France, June 1994; H. Schellman, private communication.

[15] A.J. Askew *et al.*, Phys. Lett. **B325** (1994) 212.

[16] E.A. Kuraev, L.N. Lipatov and V.S. Fadin, Sov. Phys. JETP **45** (1977) 199.
Ya.Ya. Balitsky and L.N. Lipatov, Sov. J. Nucl. Phys. **28** (1978) 822.

[17] A. De Rujula, H. Georgi and H.D. Politzer, Ann. Phys. **1103** (1977) 315.

[18] L.W. Whitlow *et al.*, Phys. Lett. **B282** (1992) 475.
L.W. Whitlow, SLAC report SLAC-357 (1990).

[19] BCDMS collaboration: A.C. Benvenuti *et al.*, Phys. Lett. **B223** (1989) 485

[20] L.V. Gribov, E.M. Levin and M.G. Ryskin, Phys. Rep. **100** (1983) 1.

[21] NMC: P. Amaudruz *et al.*, Phys. Lett. **B295** (1992) 159.

[22] H1 collaboration: V. Brisson, presented at the 27th Int. Conf. on HEP, July 1994, Glasgow, UK.

[23] ZEUS collaboration: M. Lancaster, presented at the 27th Int. Conf. on HEP, July 1994, Glasgow, UK.

[24] L.W. Whitlow, SLAC report SLAC-357 (1990).

[25] NMC: P. Amaudruz *et al.*, preprint CERN-PPE/94-32 (1994).

[26] B. Badelek and J. Kwiecinski, Nucl. Phys. **B370** (1992) 278; Phys. Rev. **D50** (1994) 4.

[27] EMC(NA28): M. Arneodo *et al.*, Nucl. Phys. **B333** (1990) 1.

Figure Captions

[1] Measurements of $F_2^p(x,Q^2)$ at large x obtained by SLAC [18] and BCDMS [19]. The latter data are normalized by a factor 0.98 as required by the global parton analysis. The broken curves are obtained using MRS(A) partons [5], and the continuous curves using MRS(A) partons modified as in (8). For these data the target mass correction (the substitution $x \to \xi$) is the dominant modification.

[2] The sea-quark distribution $x\bar{u}(x,Q^2)$ at two values of x. The upper curves correspond to MRS(A) partons, frozen at $Q^2 = 0.625$ GeV^2. The lower continuous curves correspond to MRS(A) partons with the form factor modification as in (4) and (8). Also shown for comparison (dashed curves) are the predictions of the GRV set of partons [12].

[3] (a) The values of m_0^2 obtained from fitting to E665 [14], SLAC [18] and NMC [21] measurements of $F_2^p(x,Q^2)$ at different values of x using MRS(A) partons modified as in (8). The straight line, $m_0^2 = 0.07x^{-0.37}$ GeV^2, is the least-squares fit to the values of m_0^2.
(b) As for (a), but with $\log m_0^2$ plotted as a function of $\sqrt{\log(1/x)}$. The straight line is the least squares fit, $m_0^2 = 0.015\exp[1.54\sqrt{\log(1/x)}]$ GeV^2.

[4] The description of the E665 measurements [14] of $F_2^p(x,Q^2)$ by the MRS(A) partons modified as in (8). The curves have been renormalized downwards by a factor 1.2 for the reasons described in the text.

[5] The description of the SLAC [18] and NMC [21] measurements of $F_2^p(x,Q^2)$ by the MRS(A) partons modified as in (8).

[6] Fixed-target [14, 21] and HERA [22, 23] measurements of $F_2^p(x,Q^2)$ at selected values of x, as described by MRS(A) partons modified as in (8). The predictions of the GRV parton distributions [12] are also shown (by the dotted curves) for comparison.

[7] The description of the NMC measurements [25] of F_2^n/F_2^p by MRS(A) partons (continuous curves) and by MRS(A) partons modified as in (8) - (13) (broken curves).

[8] The description of the EMC(NA28) measurements [27] of F_2^D by MRS(A) partons modified as in (8) - (13) (continuous curves). The predictions of the GRV parton distributions [12] at very low x are also shown (by the dashed curves) for

comparison. The statistical and systematic errors on the data have been combined in quadrature. There is an additional overall normalization uncertainty of $\pm 7\%$.

[9] The description of the E665 F_2^p (renormalized upwards by a factor 1.2) [14] and EMC(NA28) F_2^D [27] measurements at fixed $Q^2 \simeq 0.3$ GeV^2 by MRS(A) partons modified as in (8) - (13) (continuous curves). The unmodified MRS(A) predictions (dashed curves) and the predictions of the GRV parton distributions [12] (dotted curve) are also shown.

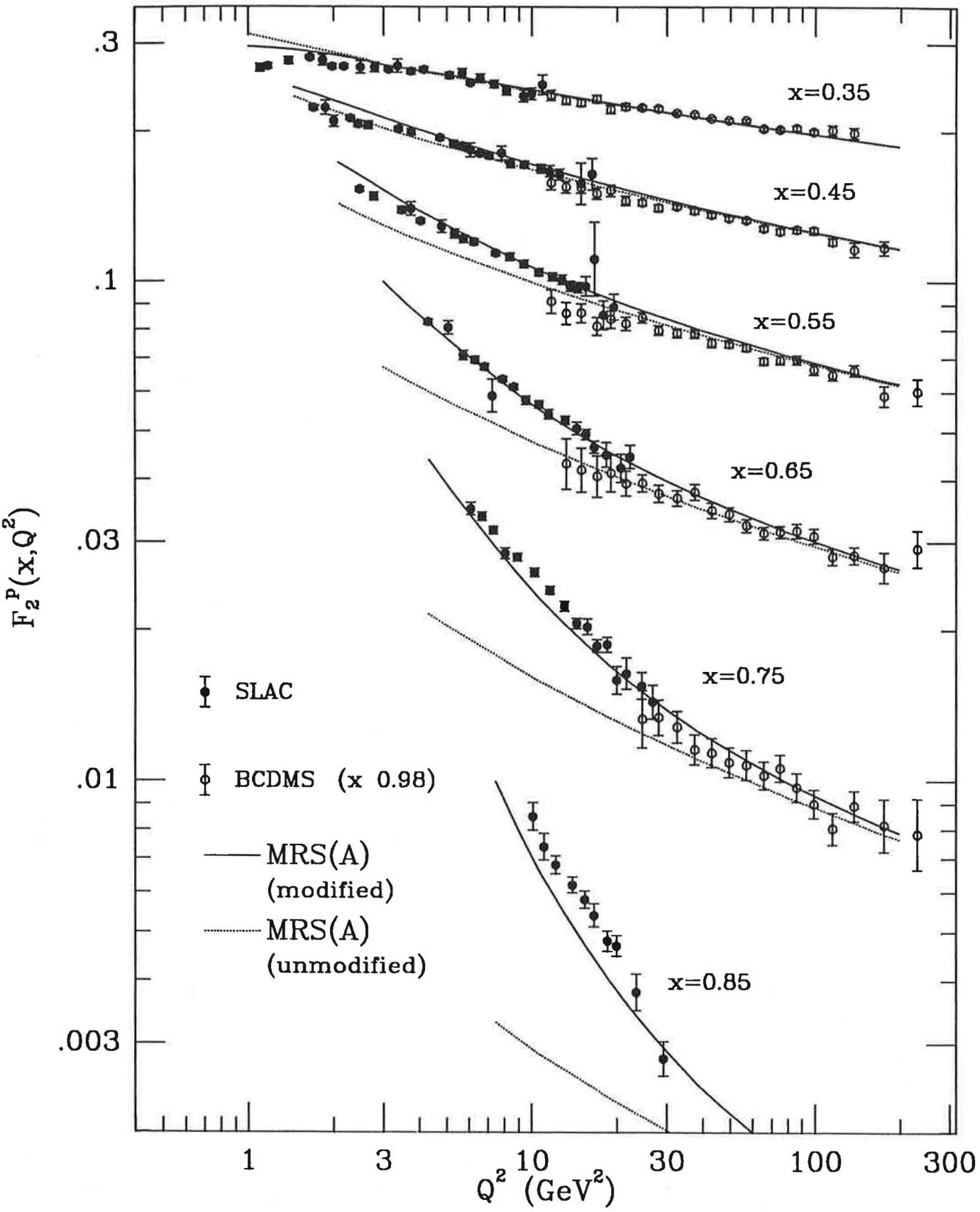
.3
.1
.03
.01
.003
$F_2^p(x,Q^2)$
x=0.35
x=0.45
x=0.55
x=0.65
x=0.75
x=0.85
SLAC
BCDMS (x 0.98)
MRS(A) (modified)
MRS(A) (unmodified)
1
3
10
30
100
300
Q^2 (GeV^2)

Fig. 1

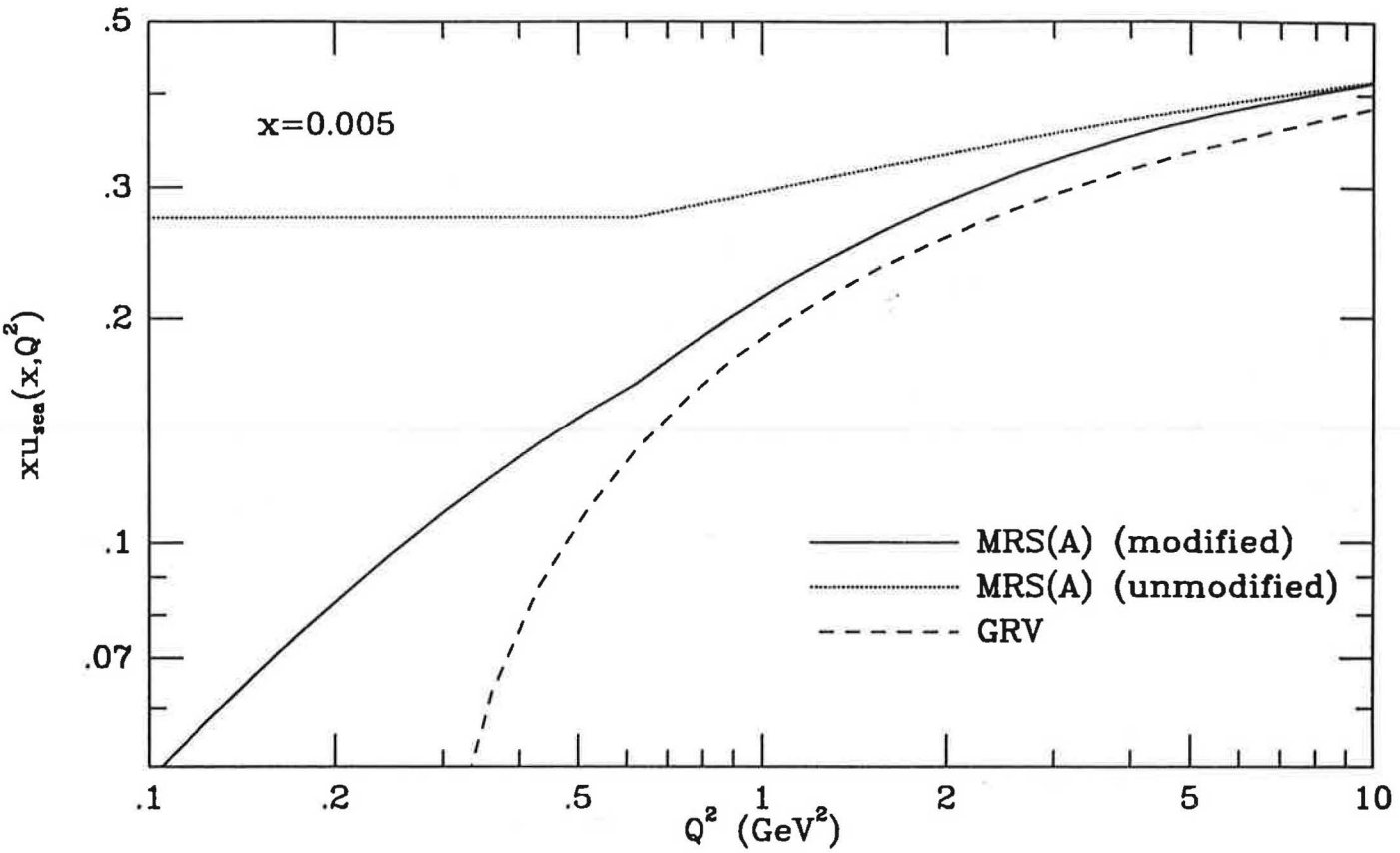
x=0.005
.5
.3
.2
.1
.07
$xu_{sea}(x,Q^2)$
MRS(A) (modified)
MRS(A) (unmodified)
GRV
.1
.2
.5
1
2
5
10
Q^2 (GeV^2)

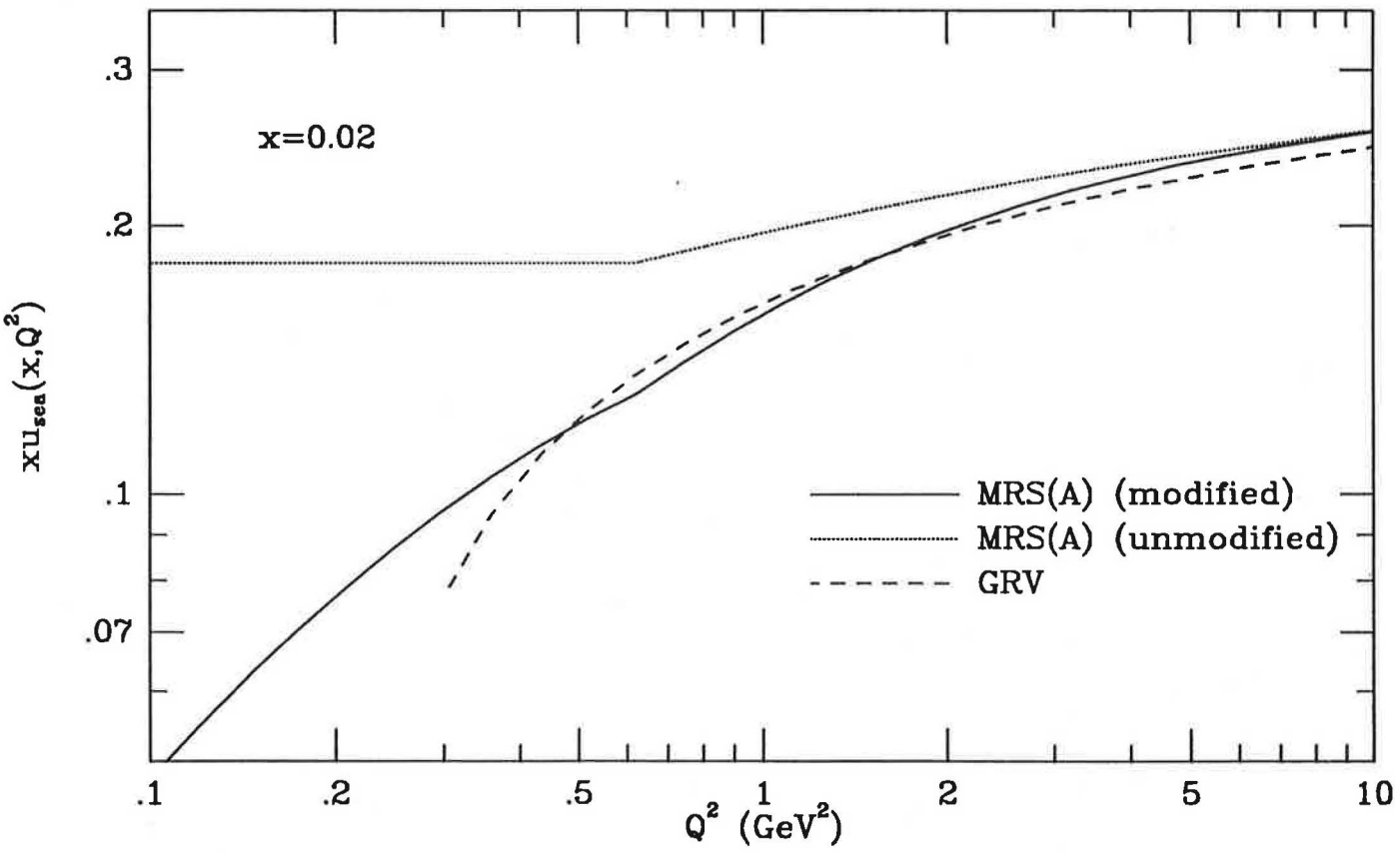
x=0.02
.3
.2
.1
.07
$xu_{sea}(x,Q^2)$
MRS(A) (modified)
MRS(A) (unmodified)
GRV
.1
.2
.5
1
2
5
10
Q^2 (GeV^2)

Fig. 2

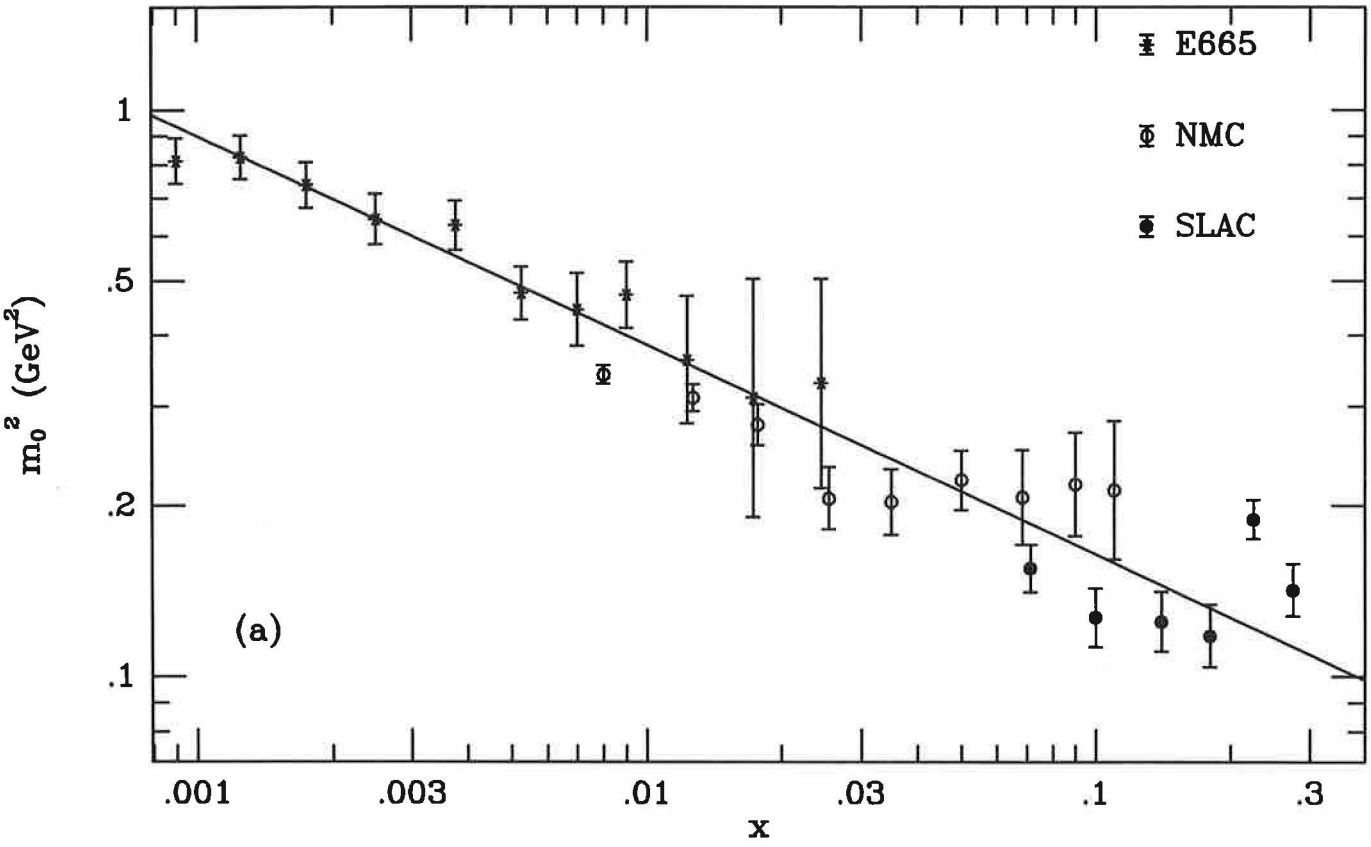
E665
NMC
SLAC
(a)
1
.5
.2
.1
m_0^2 (GeV^2)
.001
.003
.01
.03
.1
.3
x

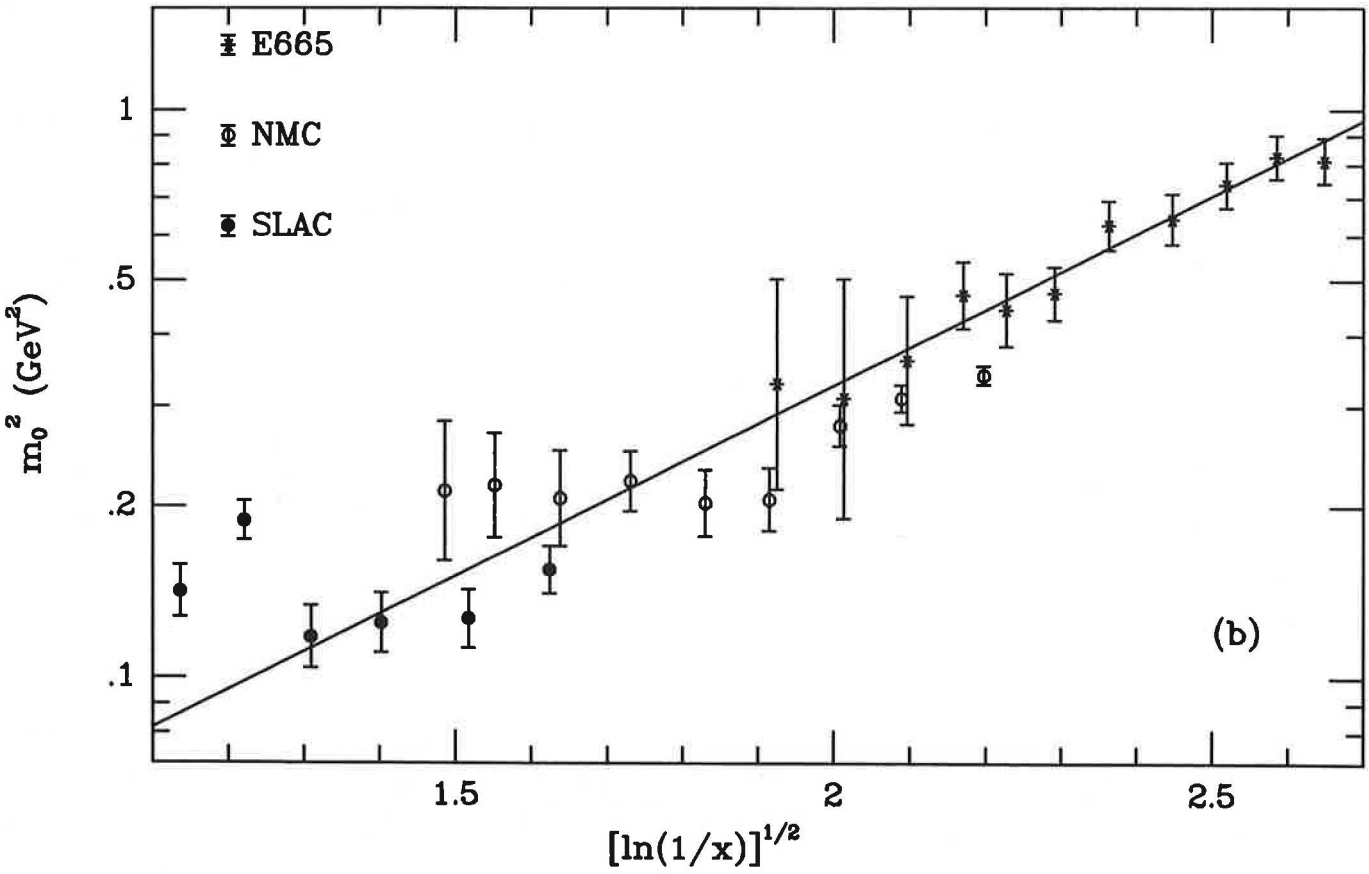
E665
NMC
SLAC
(b)
1
.5
.2
.1
m_0^2 (GeV^2)
1.5
2
2.5
$[\ln(1/x)]^{1/2}$

Fig. 3

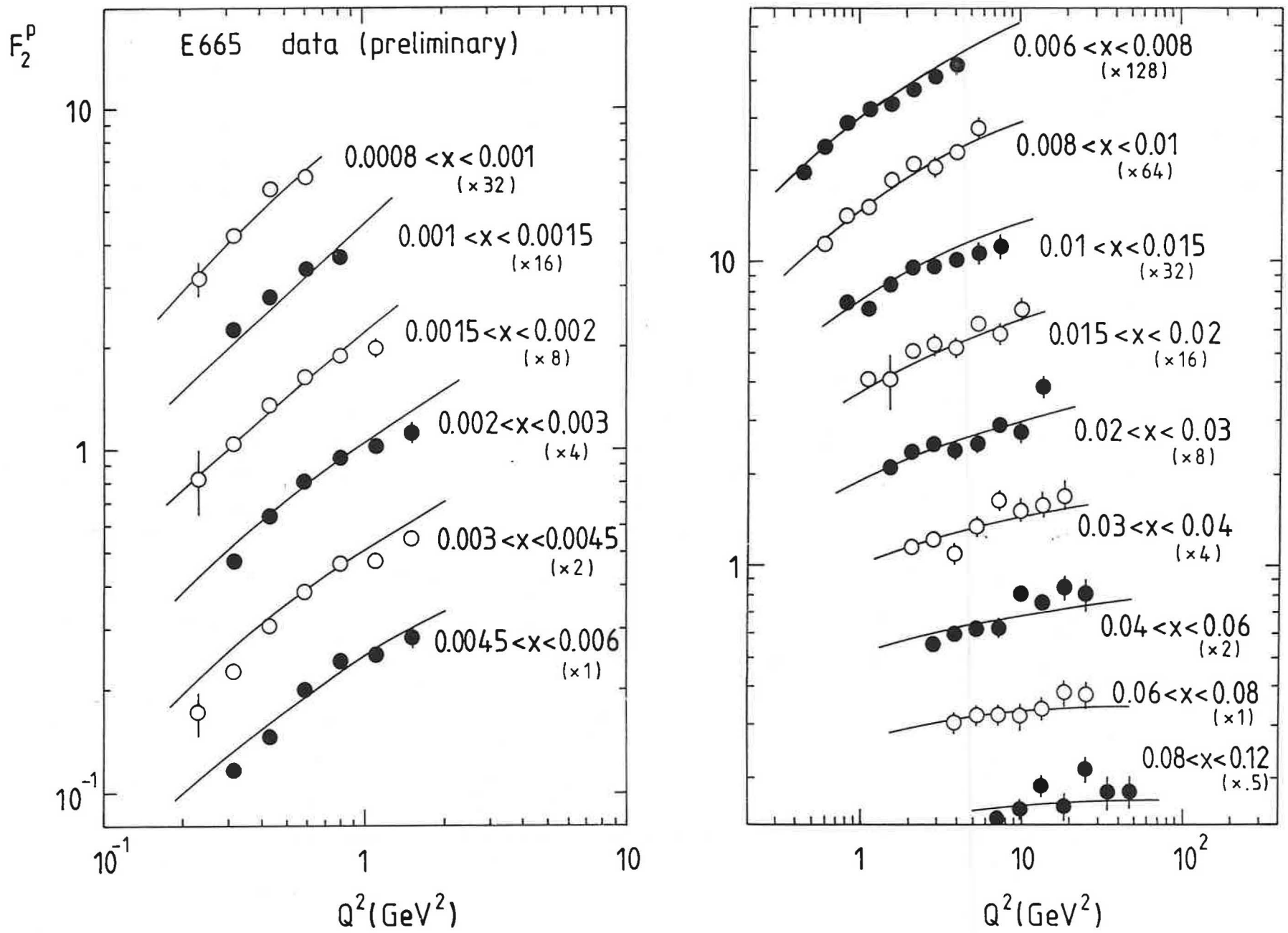
F_2^p
E665 data (preliminary)
0.0008 <x< 0.001
(×32)
0.001 <x< 0.0015
(×16)
0.0015<x< 0.002
(×8)
0.002<x<0.003
(×4)
0.003<x<0.0045
(×2)
0.0045<x<0.006
(×1)
0.006 <x< 0.008
(×128)
0.008 <x< 0.01
(×64)
0.01 <x< 0.015
(×32)
0.015 <x< 0.02
(×16)
0.02 <x< 0.03
(×8)
0.03 <x< 0.04
(×4)
0.04 <x< 0.06
(×2)
0.06<x< 0.08
(×1)
0.08<x< 0.12
(×.5)
10
1
10^{-1}
10^{-1}
1
10
10^2
$Q^2(GeV^2)$
$Q^2(GeV^2)$

Fig. 4

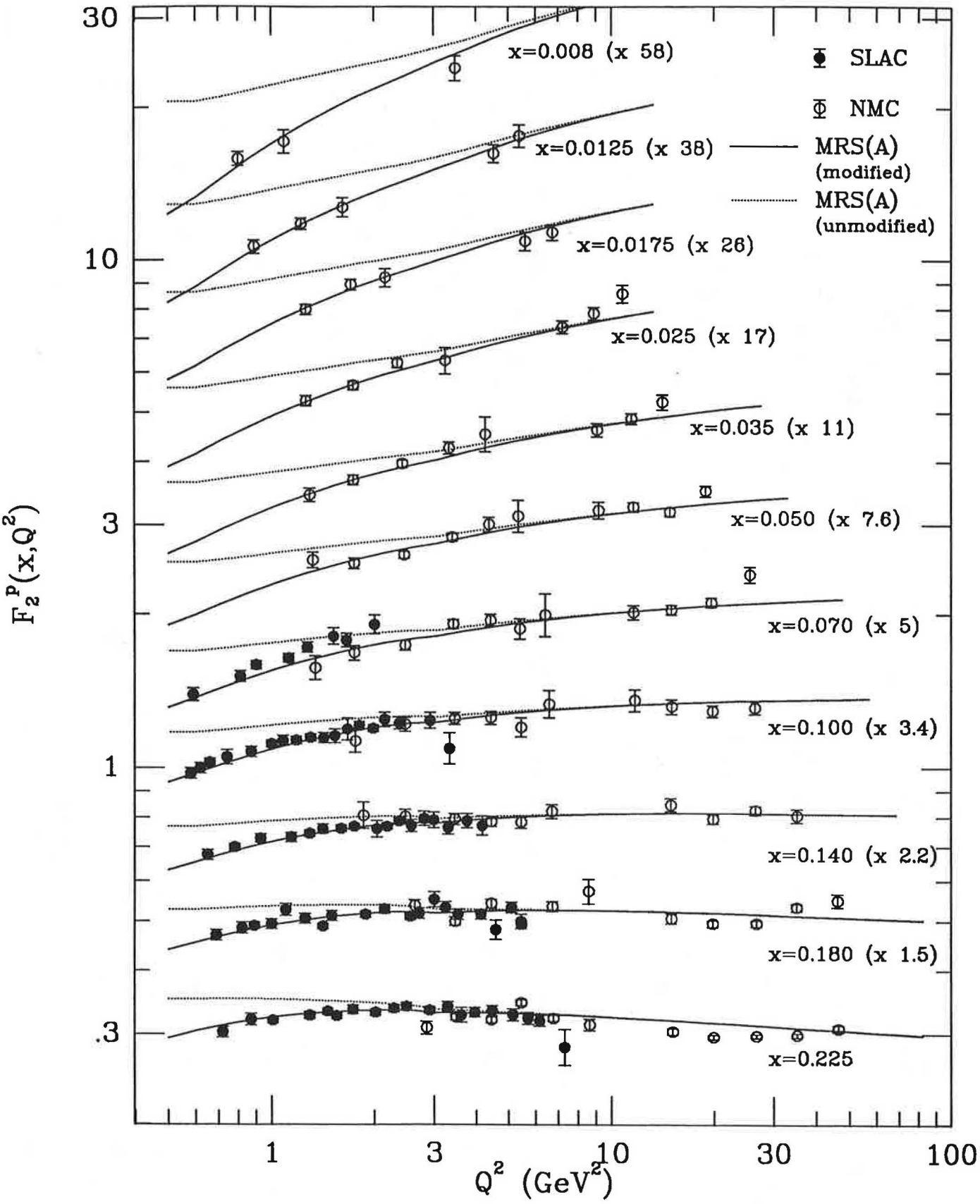
30
10
3
1
.3
$F_2^p(x,Q^2)$
x=0.008 (x 58)
x=0.0125 (x 38)
x=0.0175 (x 26)
x=0.025 (x 17)
x=0.035 (x 11)
x=0.050 (x 7.6)
x=0.070 (x 5)
x=0.100 (x 3.4)
x=0.140 (x 2.2)
x=0.180 (x 1.5)
x=0.225
SLAC
NMC
MRS(A) (modified)
MRS(A) (unmodified)
1
3
10
30
100
Q^2 (GeV^2)

Fig. 5

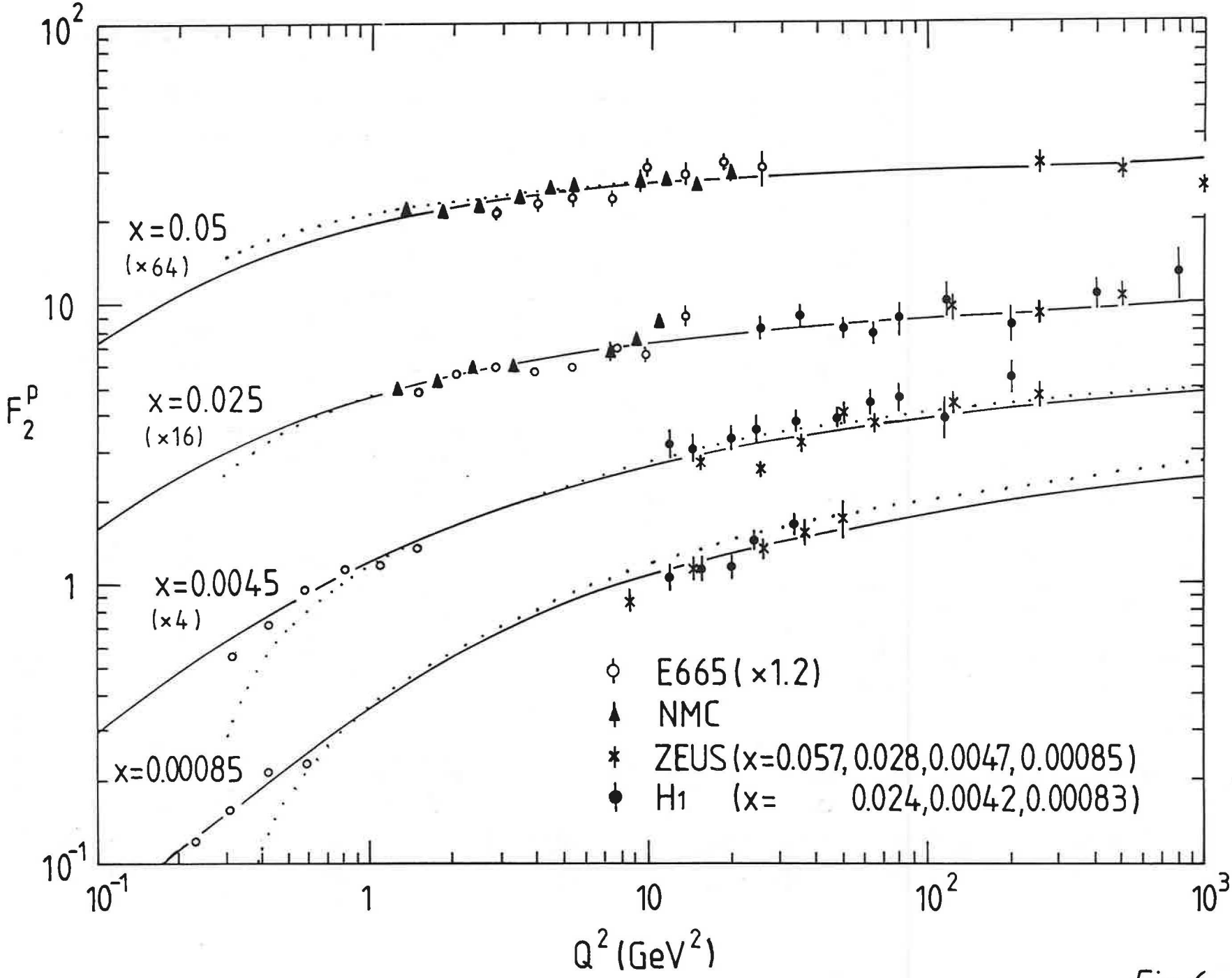
10^2
10
1
10^{-1}
F_2^p
x=0.05
(×64)
x=0.025
(×16)
x=0.0045
(×4)
x=0.00085
E665 (×1.2)
NMC
ZEUS (x=0.057, 0.028, 0.0047, 0.00085)
H1 (x= 0.024, 0.0042, 0.00083)
10^{-1}
1
10
10^2
10^3
Q^2 (GeV^2)

Fig. 6

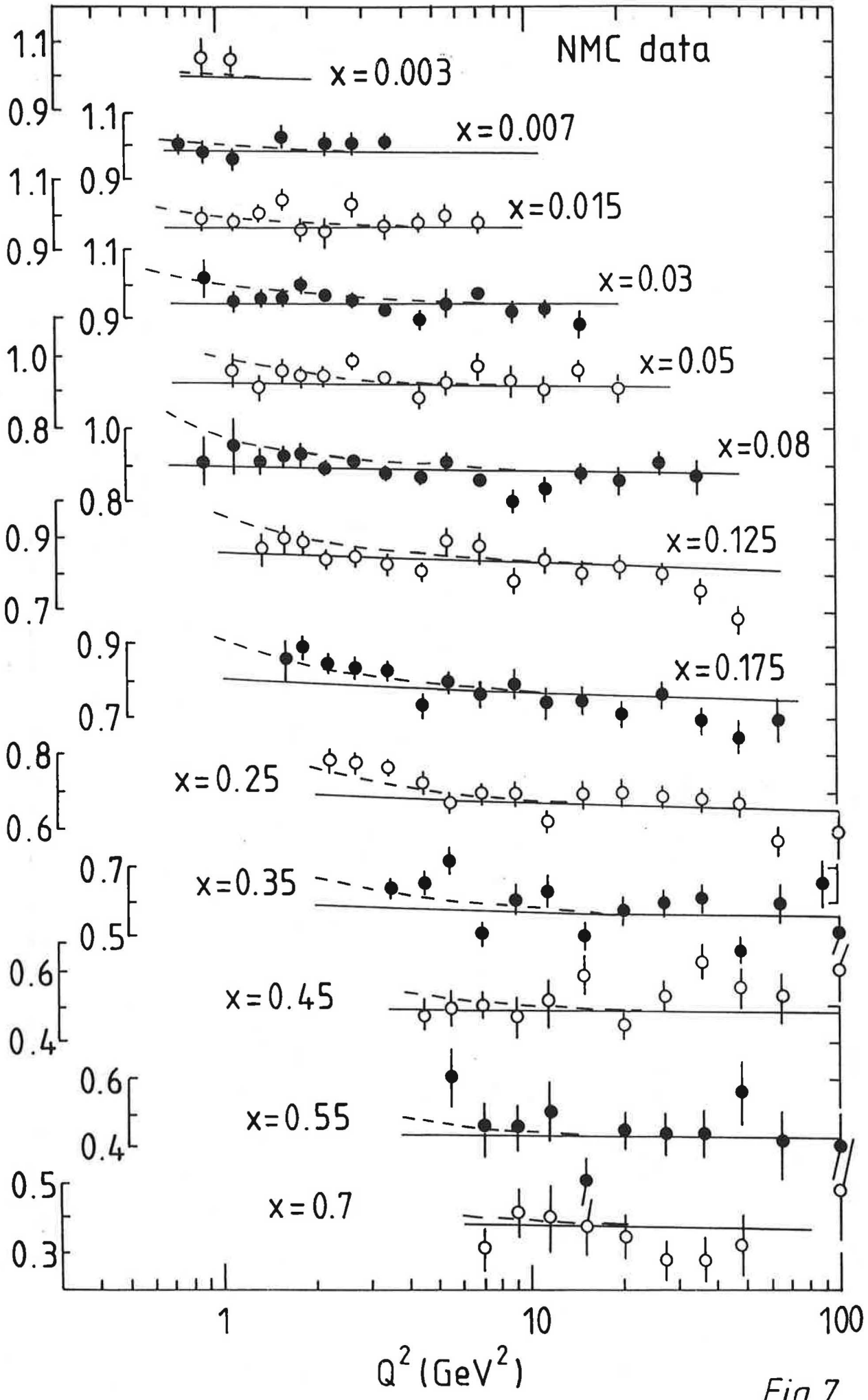
$\frac{F_2^n}{F_2^p}$
NMC data
x = 0.003
x = 0.007
x = 0.015
x = 0.03
x = 0.05
x = 0.08
x = 0.125
x = 0.175
x = 0.25
x = 0.35
x = 0.45
x = 0.55
x = 0.7
1.1
0.9
1.1
0.9
1.1
0.9
1.0
0.8
1.0
0.8
0.9
0.7
0.9
0.7
0.8
0.6
0.7
0.5
0.6
0.4
0.6
0.4
0.5
0.3
1
10
100
Q^2 (GeV^2)

Fig. 7

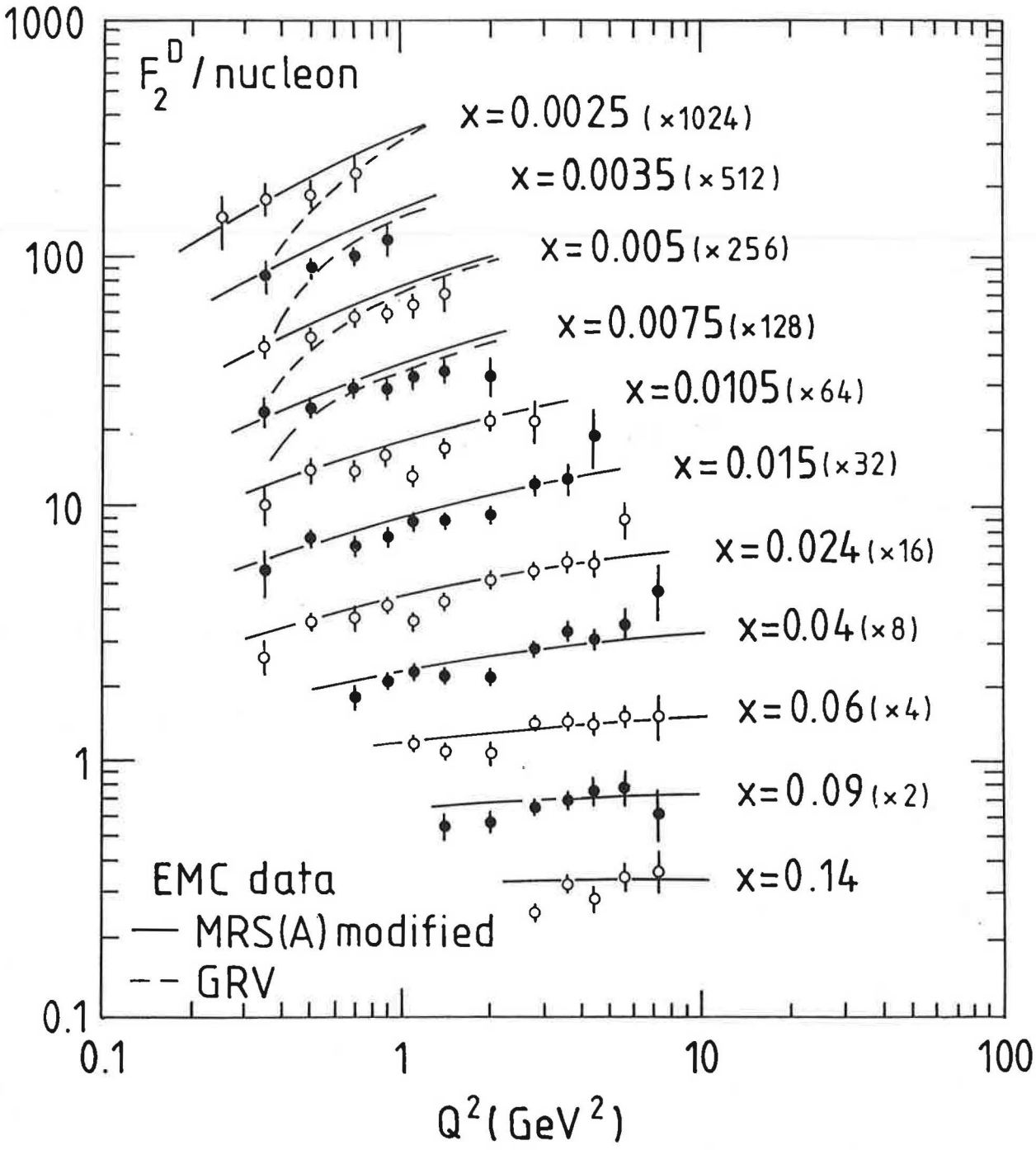
1000
100
10
1
0.1
F_2^D / nucleon
x = 0.0025 (×1024)
x = 0.0035 (×512)
x = 0.005 (×256)
x = 0.0075 (×128)
x = 0.0105 (×64)
x = 0.015 (×32)
x = 0.024 (×16)
x = 0.04 (×8)
x = 0.06 (×4)
x = 0.09 (×2)
x = 0.14
EMC data
MRS(A) modified
GRV
0.1
1
10
100
Q^2 (GeV ^{2})

Fig. 8

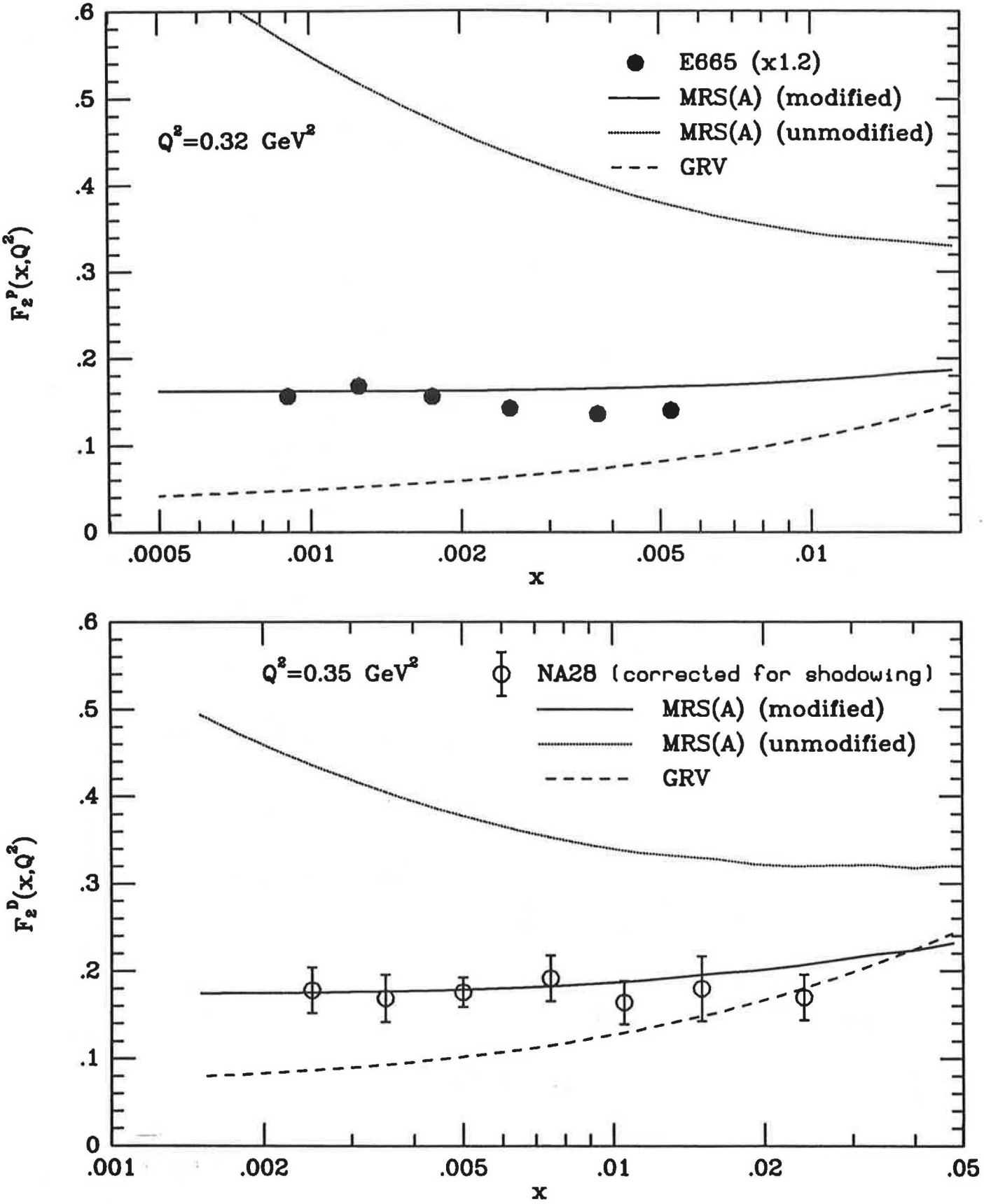
E665 (x1.2)
MRS(A) (modified)
MRS(A) (unmodified)
GRV
Q^2=0.32 GeV^2
$F_2^p(x,Q^2)$
x
.6
.5
.4
.3
.2
.1
0
.0005
.001
.002
.005
.01
Q^2=0.35 GeV^2
NA28 (corrected for shadowing)
MRS(A) (modified)
MRS(A) (unmodified)
GRV
$F_2^D(x,Q^2)$
x
.001
.002
.005
.01
.02
.05

Fig. 9